# Lattice 2019 Highlights

*Lattice 2019, Wuhan, June 2019*

*David Richards, (with help from Colin).*

# Introduction

Divide discussion into:

- Hadron Structure
- Algorithms/machines
- Weak Matrix elements
- (Spectroscopy)
- (BSM)

# Hadron Structure

# Muon g-2

- huge effort in the lattice community to calculate hadronic contributions from first principles
  $\rightarrow$ 15 parallel talks at Lattice 2019!

Vera Gulpers (Edinburgh)

## $\mu$: Experiment vs. Theory

- measured and calculated very precisely $\longrightarrow$ test of the Standard Model
- experiment: polarized muons in a magnetic field [Bennet et al., Phys.Rev. **D73**, 072003 (2006)]

$$a_\mu = 11659209.1(5.4)(3.3) \times 10^{-10}$$

- Standard Model

| | | |
|---|---|---|
| em | $(11658471.895 \pm 0.008) \times 10^{-10}$ | [K |
| weak | $(15.36 \pm 0.10) \times 10^{-10}$ | [G |
| HVP | $(693.26 \pm 2.46) \times 10^{-10}$ | [K |
| HVP($\alpha^3$) | $(-9.84 \pm 0.06) \times 10^{-10}$ | [H |
| LbL | $(10.5 \pm 2.6) \times 10^{-10}$ | [Prades et al.,Adv.Ser.Direct.High Energy Phys. 20, 303 (2009)] |

| | $\Delta a_\mu^{hvp}$ |
|---|---|
| target | $\lesssim 0.2\%$ |
| current **R**-ratio | $\approx 0.5\%$ |
| current lattice | $\approx 2-3\%$ |

- Comparison of theory and experiment: $3.8\sigma$ deviation

$$\Delta a_\mu = a_\mu^{exp} - a_\mu^{SM} = 27.9(6.3)^{Exp}(3.6)^{SM} \times 10^{-10}$$

| | | |
|---|---|---|
| required precision to match upcoming experiments | $\Delta a_\mu^{hvp} \lesssim 0.2\%$ | $\Delta a_\mu^{lbl} \lesssim 10\%$ |

Hadronic Vacuum Polarisation

### Hadronic Vacuum Polarisation (HVP) from the R-ratio

- current best theoretical estimate uses experimental data
- optical theorem


- R-ratio

$$R(s) = \frac{\sigma(e^+e^- \to \text{hadrons}, s)}{\sigma(e^+e^- \to \mu^+\mu^-, s)}$$

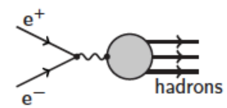


$$a_\mu^{hvp} = \left(\frac{\alpha m_\mu}{3\pi}\right)^2 \int_{m^2}^{\infty} ds \frac{R(s)K(s)}{s^2}$$

re

$\approx$

# g-2 - II



## Hadronic Vacuum Polarisation (HVP) from the Lattice

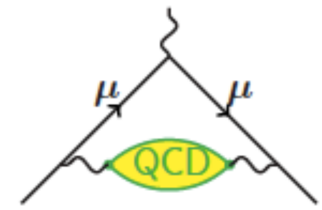


- $\Pi_{\mu\nu}(Q) \equiv \int d^4x\, e^{iQ\cdot x} \left\langle j^\gamma_\mu(x)\, j^\gamma_\nu(0) \right\rangle = (Q_\mu Q_\nu - \delta_{\mu\nu} Q^2)\, \Pi(Q^2)$
- electromagnetic current $\quad j^\gamma_\mu = \frac{2}{3}\bar{u}\gamma_\mu u - \frac{1}{3}\bar{d}\gamma_\mu d - \frac{1}{3}\bar{s}\gamma_\mu s + \frac{2}{3}\bar{c}\gamma_\mu c$
- hadronic contribution to the anomalous magnetic moment of the muon
  [ T. Blum, Phys.Rev.Lett.91, 052001 (2003)]

$$a_\mu^{hvp} = \left(\frac{\alpha}{\pi}\right)^2 \int_0^\infty dQ^2\, K(Q^2)\, \hat{\Pi}(Q^2) \qquad \text{with} \quad \hat{\Pi}(Q^2) = 4\,\pi^2 \left[\Pi(Q^2) - \Pi(0)\right]$$

- subtracted HVP from vector correlator [Bernecker and Meyer, Eur.Phys.J. **A47**, 148 (2011)]

$$C(t) = \frac{1}{3}\sum_{k=0}^{2}\sum_{\vec{x}} \langle j^\gamma_k(\vec{x},t) j^\gamma_k(0)\rangle \qquad \hat{\Pi}(Q^2) = 4\pi^2 \int_0^\infty dt\, C(t) \left[\frac{\cos(Qt)-1}{Q^2} + \frac{1}{2}t^2\right] \qquad a_\mu^{hvp} = \int_0^\infty dt\, f(t) C(t)$$

- flavour decomposition (isospin symmetric QCD)

$$C(t) = \frac{5}{9}C^\ell(t) + \frac{1}{9}C^s(t) + \frac{4}{9}C^c(t) + C^{disc}(t)$$

# g-2 - III

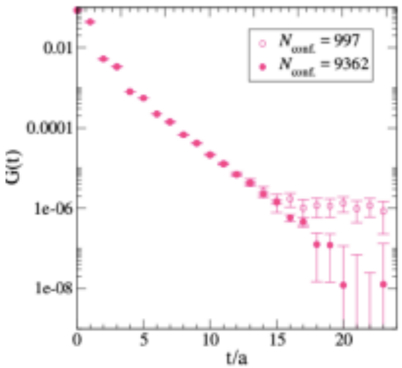


[C. Davies *et al*, arXiv:1902.04223]

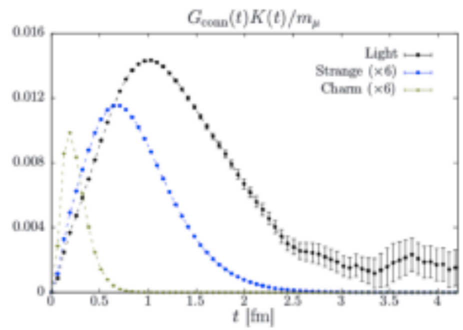


[A. Gérardin *et al*, arXiv:1904.03120]

- Dominated by 2-pion at large *t.*

▸ study using ensembles with different volumes

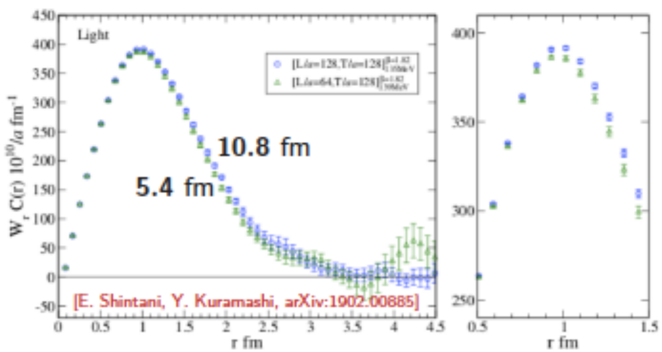


[E. Shintani, Y. Kuramashi, arXiv:1902.00885]

$\rightarrow$ FV effects about **1.7**× larger than NLO ChiPT

▸ ETMC [D. Giusti, *et al*, Phys. Rev. D 98, 114504 (2018)]
GS and perturbative QCD for small **t**

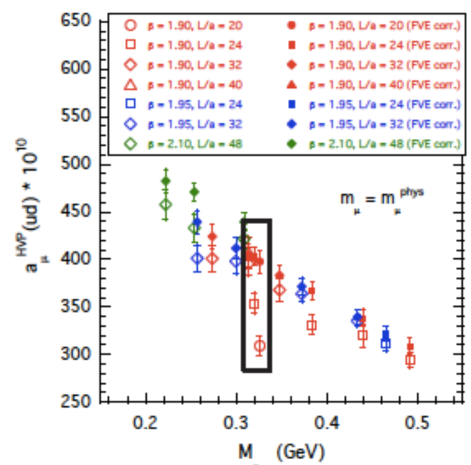

# g-2 - IV



## Full HVP comparison

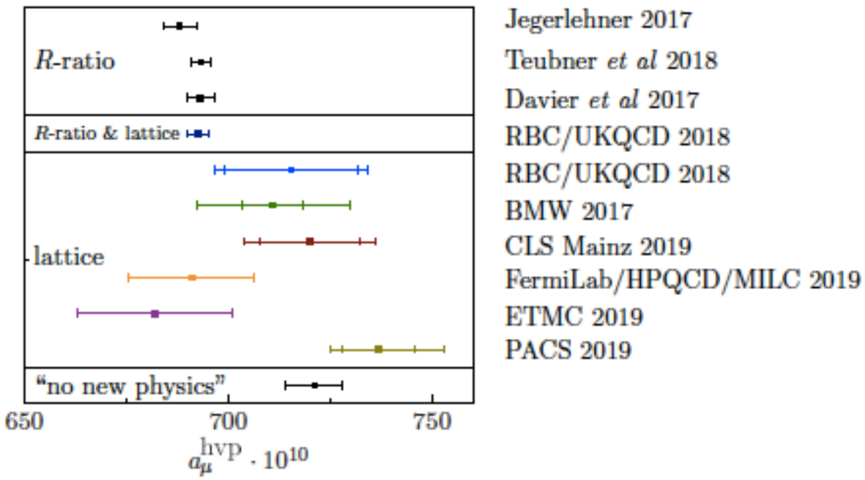


contribution to $a_\mu^{\mathrm{hvp}}$

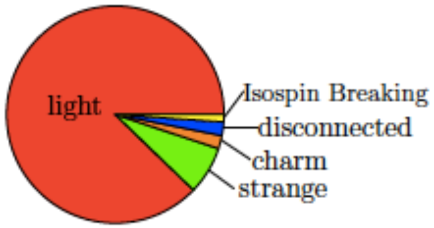


contribution to $\Delta a_\mu^{\mathrm{hvp}} \approx 2.5\%$

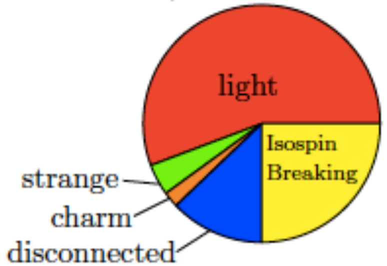

# Wilson Award

Luchang Jin
University of Connecticut / RIKEN BNL Research Center

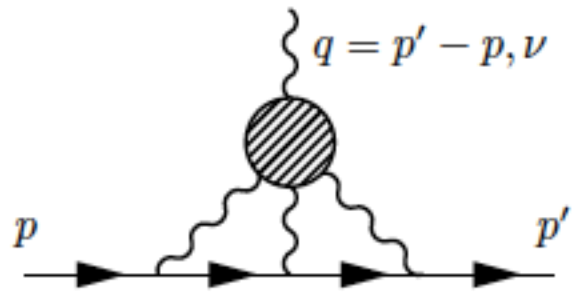


QED + QCD

HLbL: Hadronic Light by Light

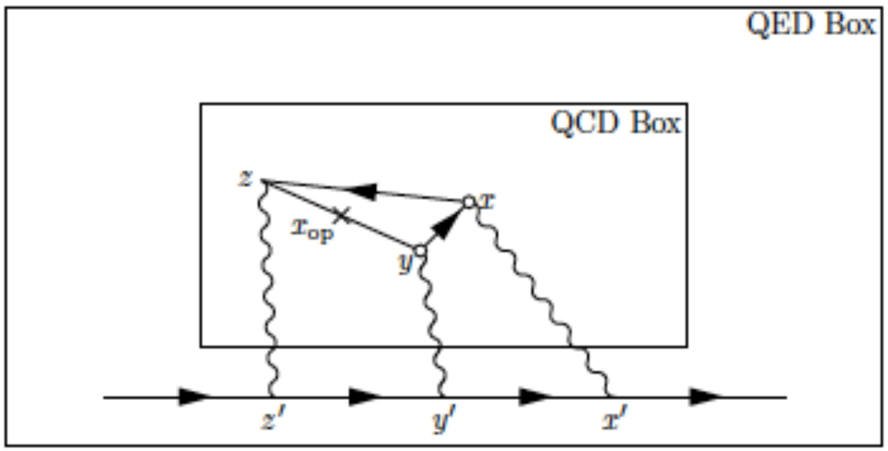


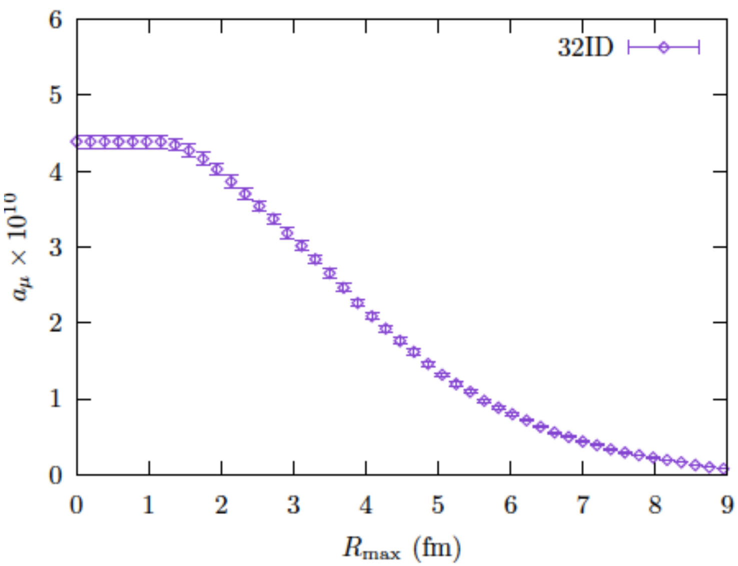

# Wilson Award - II

## Pion mass splitting: $M_{\pi^+} - M_{\pi^0}$ (prelim)



$$\Delta M_\pi^2(a, M_\pi) = 2M_\pi \Delta M_\pi = \Delta M_\pi^2(0, M_{\pi^+}^{\text{phys}}) + c_1 a^2 + c_2(M_\pi^2 - (M_{\pi^+}^{\text{phys}})^2)$$

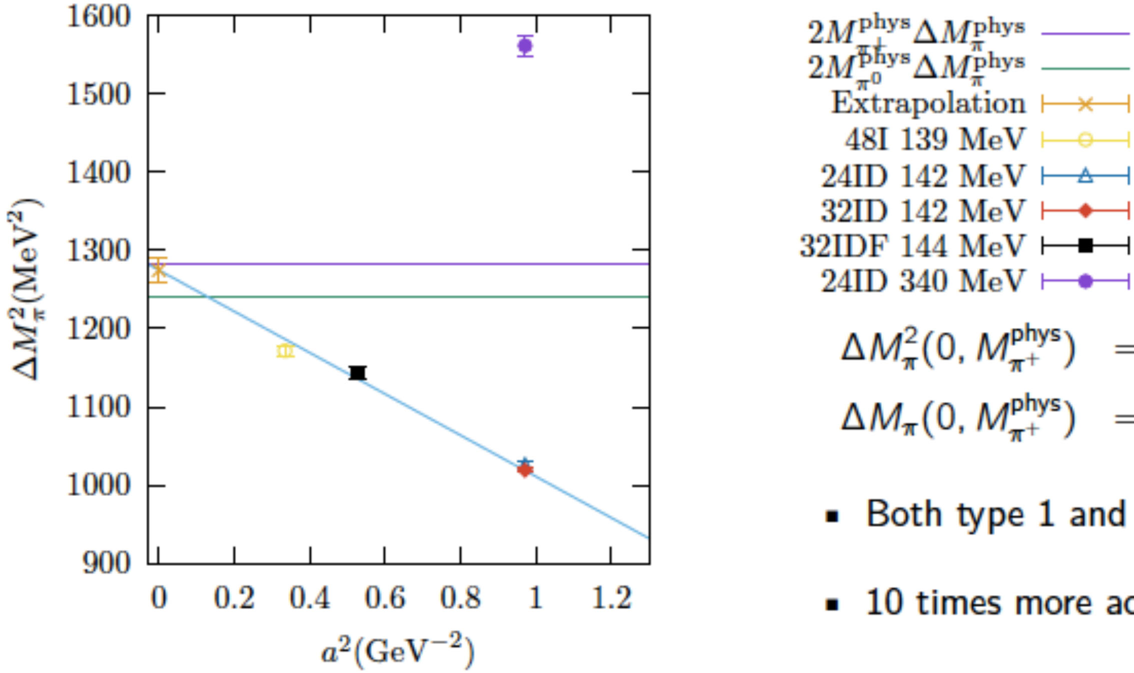


$$\Delta M_\pi^2(0, M_{\pi^+}^{\text{phys}}) = 1.275(15) \times 10^3 \text{ MeV}$$

$$\Delta M_\pi(0, M_{\pi^+}^{\text{phys}}) = 4.57(6) \text{ MeV}$$

- Both type 1 and type 2 diagrams included.
- 10 times more accurate than previous.

# Nucleon Structure - Charges

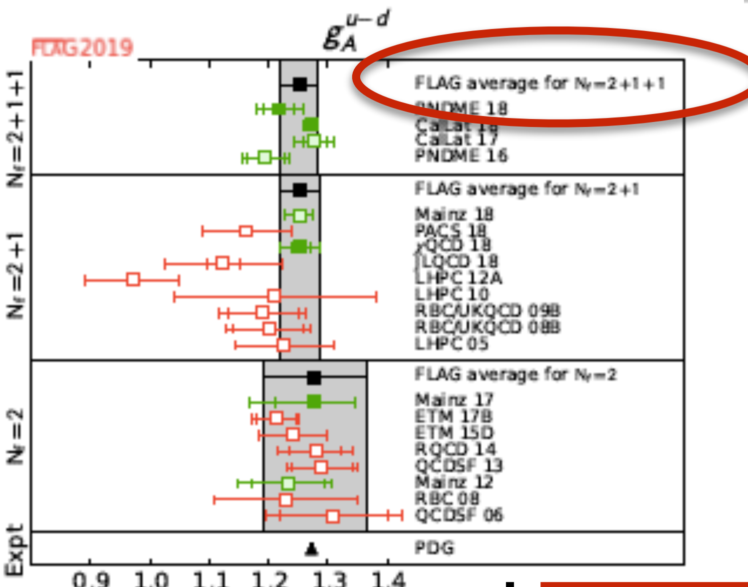


Tanmoy Bhattacharya

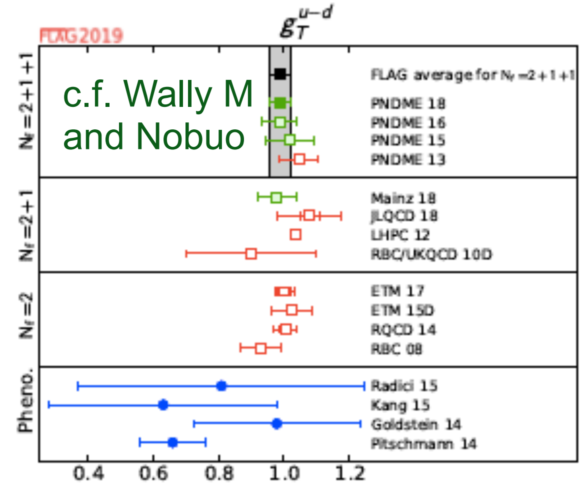


c.f. Wally M and Nobuo

Andre Walker-Loud

Nature 558 (2018) no. 7708, 91-94
Chang et al. [arXiv:1805.12130]

1 year on Titan (ORNL) + 2 years on GPU machines at LLNL

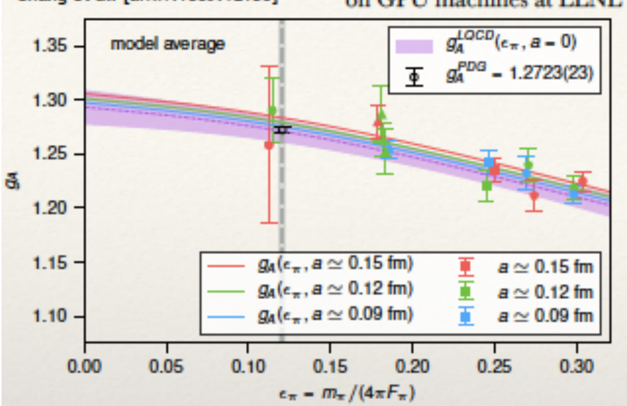


Sierra Early Science

PRELIMINARY

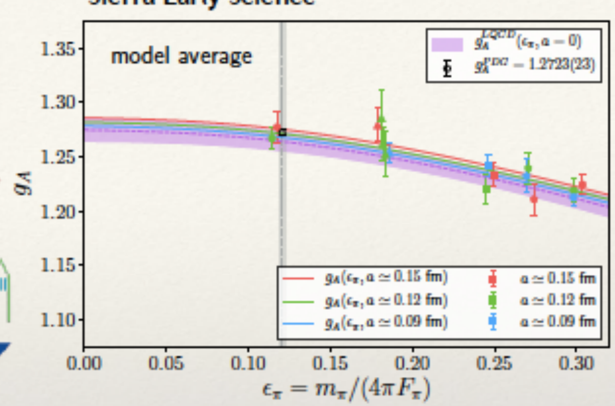

# Flavor-separated

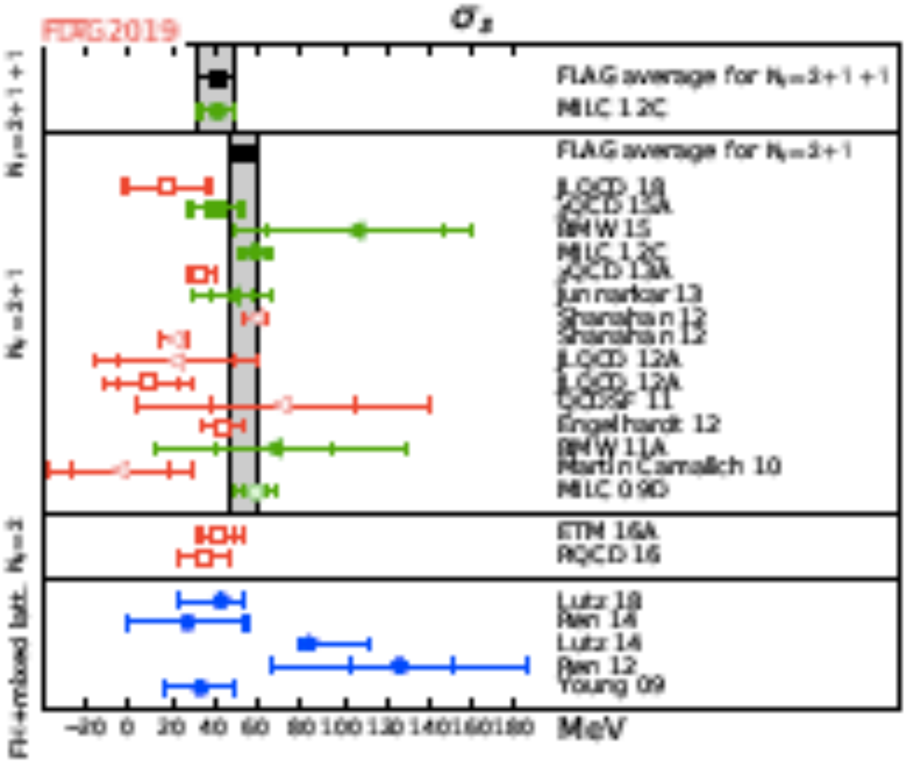

# Nucleon - Form Factors

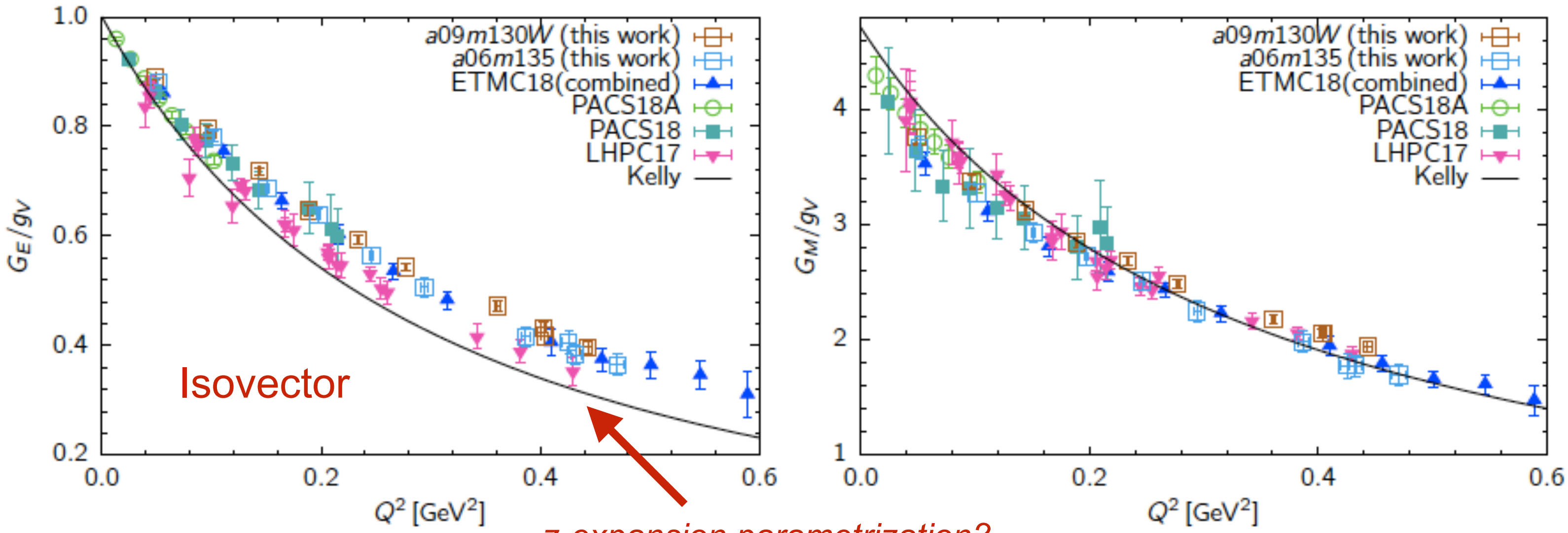


*z-expansion parametrization?*

Tanmoy Bhattacharya

# Nucleon Charge Radius

$$\frac{\partial}{\partial k^2} C_{2\text{pt}}(t) = \int d^3x \langle N_{t,x} | N^\dagger_{0,0} \rangle \frac{-ix_i}{2k} e^{-ikx_i}$$

$$\lim_{k^2 \to 0} C'_{2\text{pt}}(t) = \int d^3x \langle N_{t,x} | N^\dagger_{0,0} \rangle \frac{-x_i^2}{2}$$

C. Bouchard, KO, DGR

$$\frac{\partial}{\partial k^2} C_{3\text{pt}}(T,t') = \int d^3x d^3x' \langle N_{T,x} | \Gamma_{t'x'} | N^\dagger_{0,0} \rangle \frac{-ix'}{2k} e^{-ikx'_i}$$

$$\lim_{k^2 \to 0} C'_{3\text{pt}}(T,t') = \int d^3x d^3x' \langle N_{T,x} | \Gamma_{t'x'} | N^\dagger_{0,0} \rangle \frac{-x'^2}{2}$$

Jason Chang

**Moment methods**

Description of finite-volume contributions

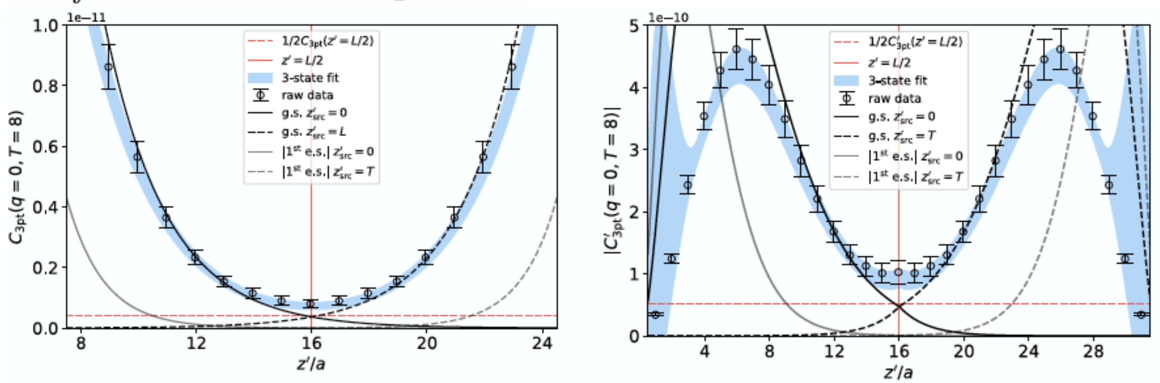


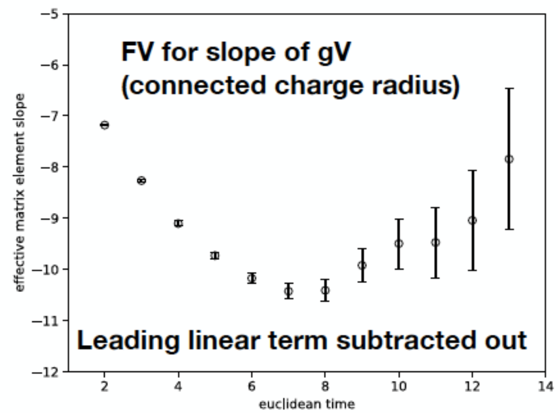


Plateau in *slope*

# Axial-Vector Form Factor

$$\langle N|A_\mu|N\rangle \equiv \bar{u}\left[G_A\gamma_\mu + \tilde{G}_P\frac{q_\mu}{2M}\right]\gamma_5 u \qquad \langle N|P|N\rangle \equiv \bar{u}G_P\gamma_5 u$$

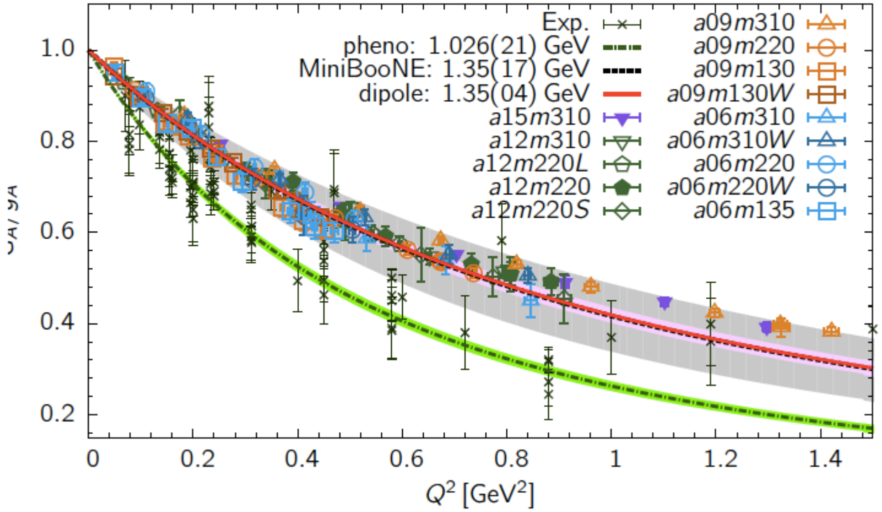


Tanmoy Bhattacharya

Also new results (Wilhelm) for $G_A^s$.

Oliver Baer

$N\pi$ contamination in $G_P(Q^2)$

for $t$ = 1.3 fm

PACS plateau estimate data for normalized form factor independent of $Z_P$

$$G_P^{\rm norm}(Q^2, Q^2_{\rm ref}, t) \equiv \frac{G_P^{\rm plat}(Q^2, t)}{G_P^{\rm plat}(Q^2_{\rm ref}, t)}$$

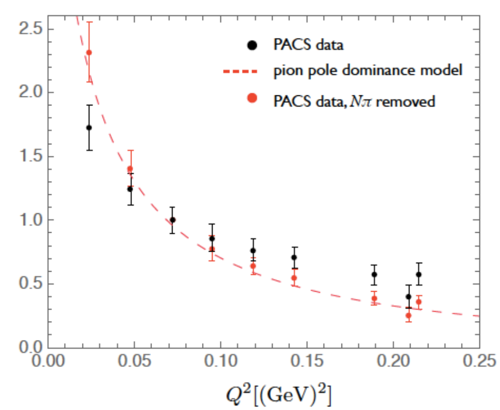

# PDFs

- Topic close to my heart… ….many references to Karpie et al

## Large-momentum effective theory

$$\lim_{P^z \to \infty} \tilde{q}(x, P^z, \mu) = q(x, \mu)?$$ ✗

Yong Zhao

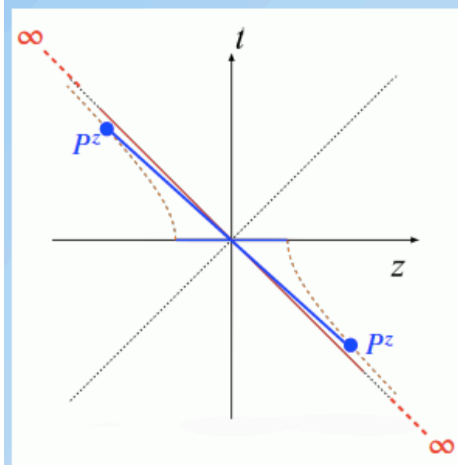


Instead of taking $P^z \to \infty$ limit, one can perform an expansion for large but finite $P^z$:

$$\tilde{q}(x, P^z, \mu) = \int \frac{dy}{|y|} C\left(\frac{x}{y}, \frac{\mu}{yP^z}\right) q(y, \mu) + O\left(\frac{M^2}{P_z^2}, \frac{\Lambda_{\rm QCD}^2}{x^2 P_z^2}\right)$$

- Ji, PRL110 (2013);
- X. Xiong, X. Ji, J.-H. Zhang and Y.Z., PRD90 (2014);
- Y.-Q. Ma and J. Qiu, PRD98 (2018), PRL 120 (2018);
- T. Izubuchi, X. Ji, L. Jin, I. Stewart, and Y.Z., PRD98 (2018).

- $\tilde{q}(x, P^z)$ and $q(x)$ have the same infrared physics (nonperturbative), but different ultraviolet (UV) physics (perturbative);
- Therefore, the matching coefficient $C$ is perturbative, which controls the logarithmic dependences on $P^z$.

# PDFs - II

Recent strategies to reconstruct PDF from lattice

Nikhil Karthik

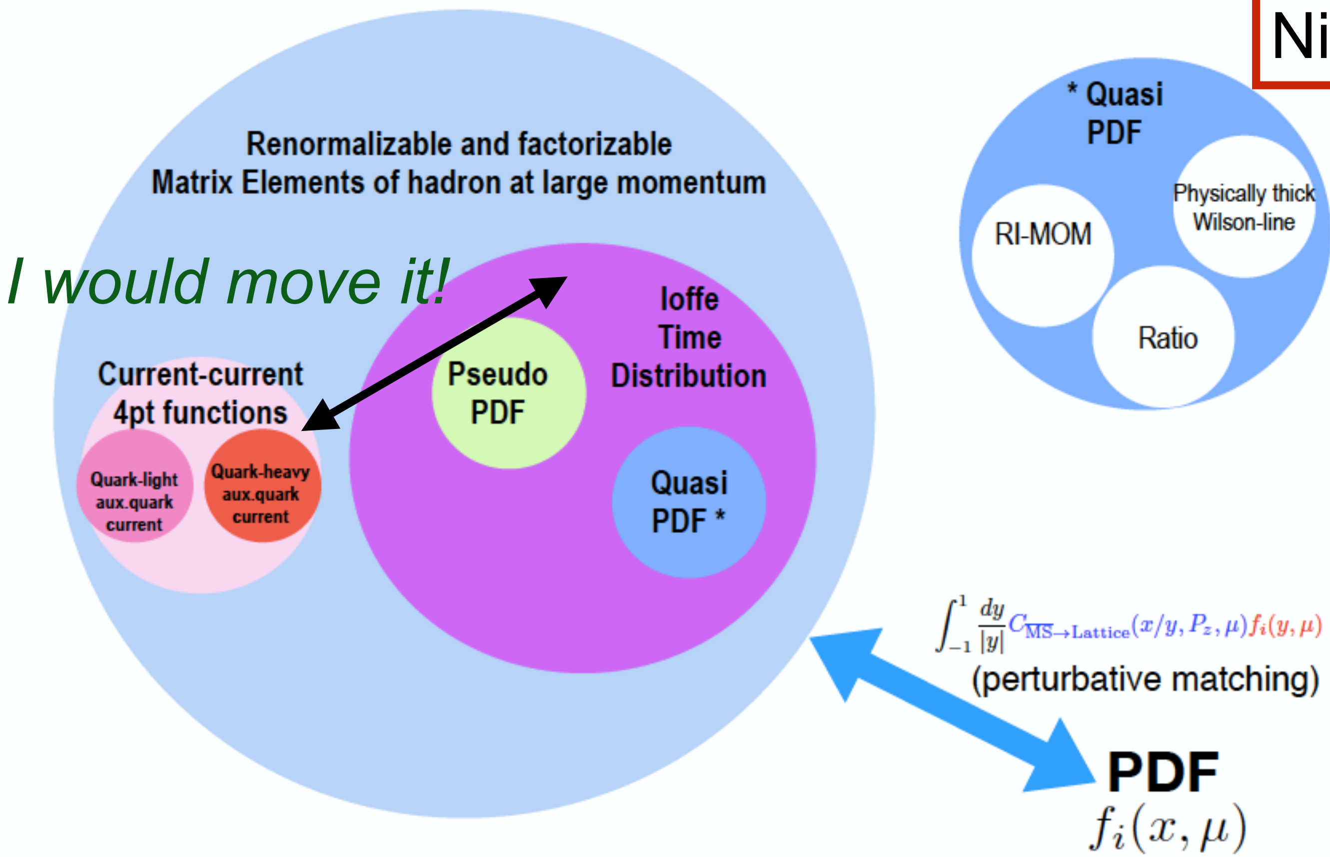


Y.Q.Ma and J.W.Qiu, PRL120 (2018),022003

A. Radyushkin, PRD98 (2017),034025

X. Ji, PRL110 (2013), 262002

W. Detmold and C.J. D. Lin, PRD73 (2006) 014501
V. M. Braun and D. Muller, EPJ C55, 349 (2008)

R.S. Sufian et al, PRD (2019), 074507

# PDFs - III

$$\frac{\langle H(t_{\rm sink})\, \overline{\psi}(0) \, W(0,z) \, \gamma_t\psi(z)\, H^\dagger(0)\rangle}{\langle H(t_{\rm sink}) H^\dagger(0)\rangle}$$

$t_{\rm sink} \to \infty$

$$h(z, P_z) = \langle P_z | \overline{\psi}(0) \, W(0,z) \, \gamma_t\psi(z) | P_z \rangle$$

Renormalize

$h^R(z, P_z, P^R)$ $\qquad$ $\mathcal{M}(zP_z, z^2) = \dfrac{h(z, P_z)}{h(z,0)}$ **Reduced Ioffe time distribution**

Fourier z to conjugate x at fixed $P_z$ $\qquad$ Fourier $zP_z$ to conjugate x at fixed $z^2$

**Quasi-PDF** $\tilde{q}(x, P_z, P^R)$ $\qquad$ $\tilde{\mathcal{M}}(x, z^2)$ **pseudo-PDF**

LaMET $\qquad$ Light-ray OPE

**Lattice cross-section e.g.,**

$$f(x, \mu^2) \longleftarrow\!/\!/\!\!-\!\!- \langle P_z | j_V(0) \quad j_A(z) | P_z \rangle$$

**From lattice correlator to PDF**

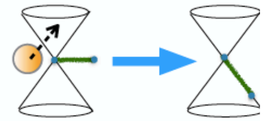

*Need to reach high momenta*

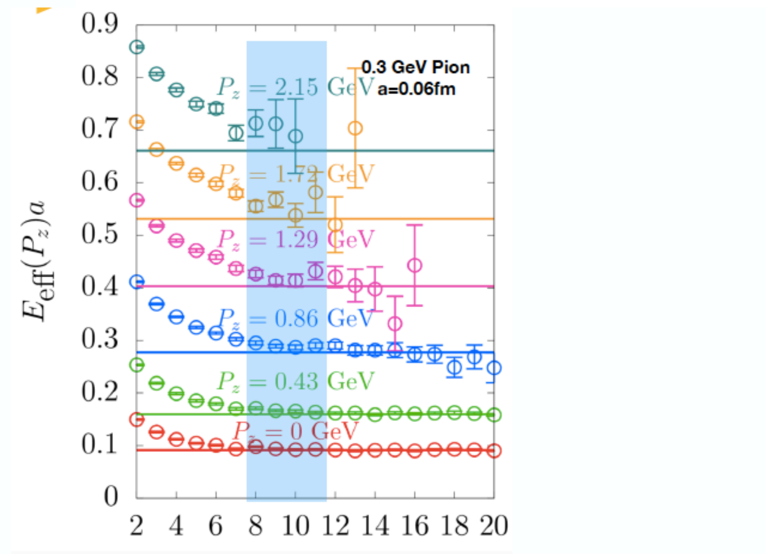


(BNL-SBU-U.Conn) T.Izubuchi et al, arXiv:1905.06349

# Does it make sense?

## Check OPE relations directly

$$\frac{\partial^n}{\partial \nu^n}\mathcal{M}(\nu,z^2)\big|_{\nu=0} = c_n(z^2\mu^2)\frac{\partial^n}{\partial \nu^n}M(\nu,\mu^2)\big|_{\nu=0}$$

Reduced (renormalized) Ioffe time distribution

Wilson-coeff

Light-cone Ioffe time distribution

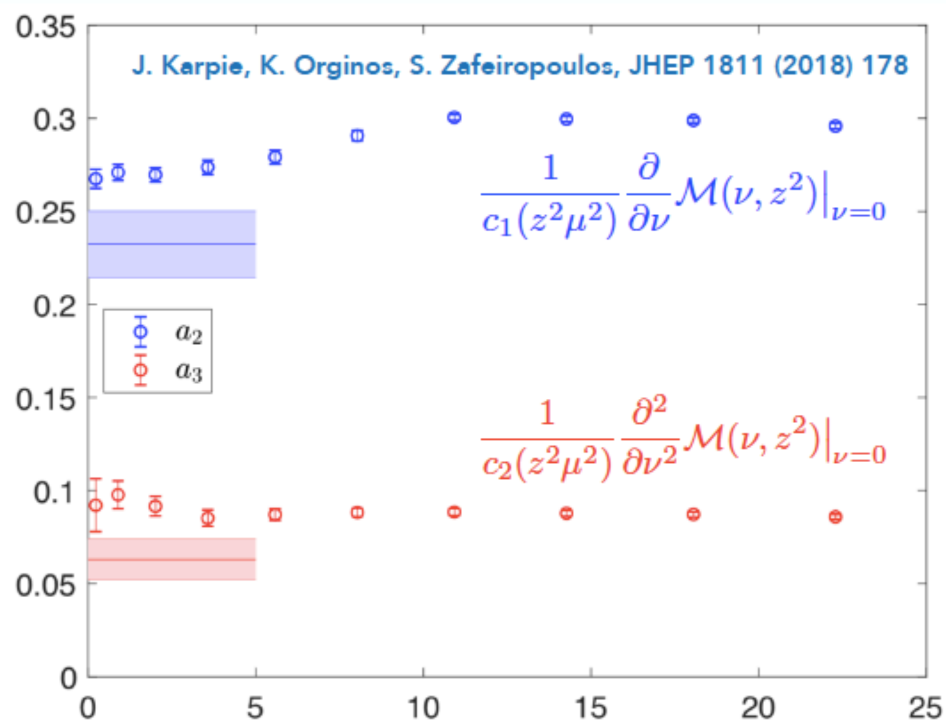


- Lattice spacing divergences

  X by Z-factor
- Diverging moments of renormalized quasi/pseudo-PDFs.

  X by $z \to 0$ divergence of $C_n$

# Solution of inverse problem

Paradigm

Short distance scale

$$\sigma_n(\omega,\xi^2,P^2) = \sum_a \int_{-1}^{1} \frac{dx}{x} f_a(x,\mu^2) K_n^a(x\omega,\xi^2,x^2P^2,\mu^2) + \mathcal{O}(\xi^2\Lambda^2_{\mathrm{QCD}})$$

*Calculated in LQCD*

Parton Distribution function

*Calculated in perturbation theory ("process dependent")*

(Model) dependence on how Fourier transform is truncated

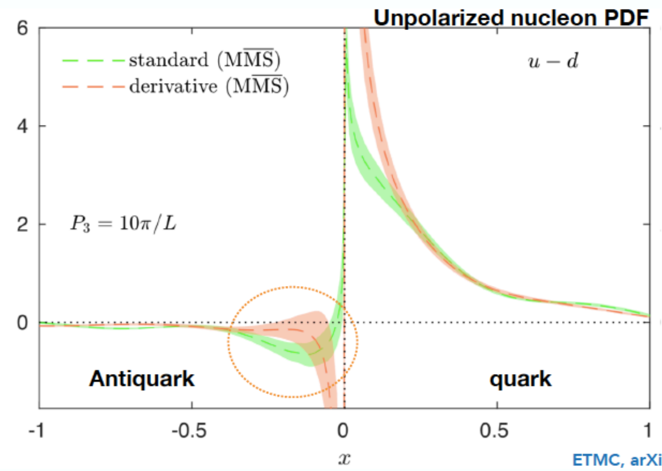


EMTC studies: Krzystof Cichy Wednesday 9:40

ETMC, arXiv:1902.00587
ETMC, PRL. 121 (2018), 112001
LP3, arXiv:1803.04393

The conclusions on $\bar{u}$-$\bar{d}$ asymmetry in nucleon sea is dependent on method

Model-independent neural-network approach

J. Karpie, K. Orginos, A. Rothkopf, S. Zafeiropoulos, JHEP 1904 (2019) 057

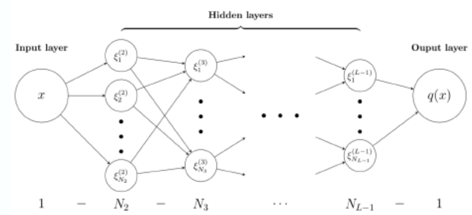

# Pion PDF - I

- Parameterize PDF via

$$f(x; a, b) = N(a, b)x^a(1-x)^b; \;\; N(a, b) = \frac{\Gamma(a+b+2)}{\Gamma(a+1)\Gamma(b+1)}$$

C. Shugert

Quasi-PDF Results

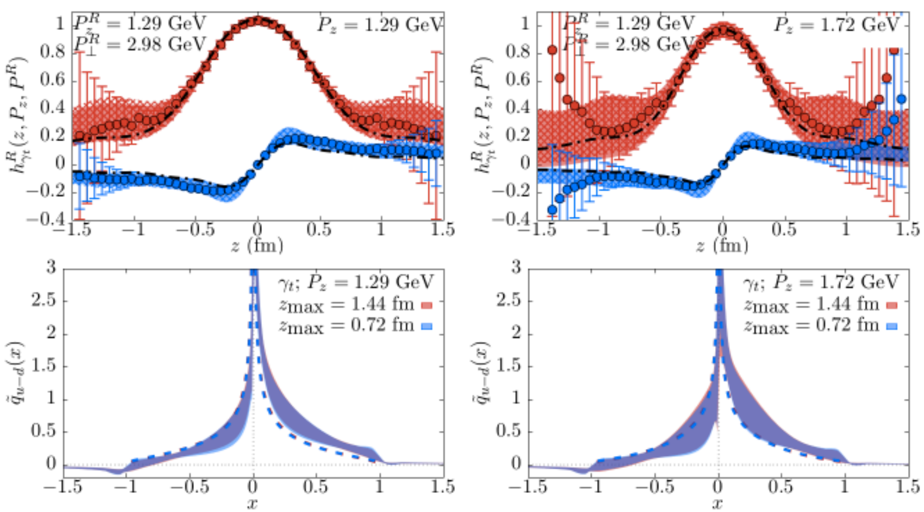


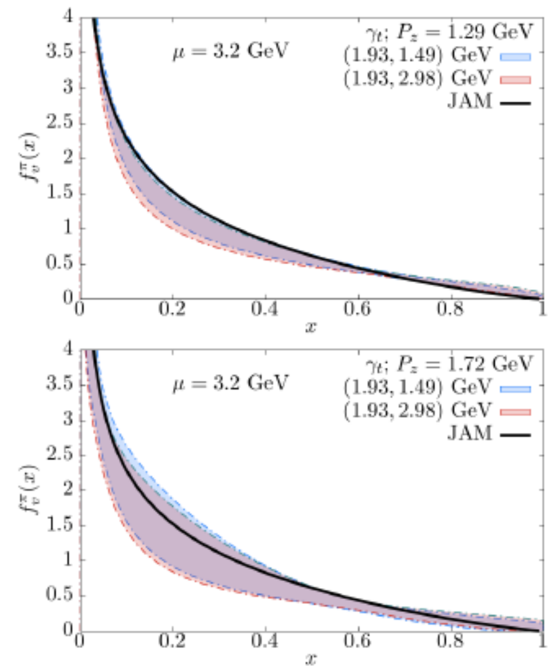

# Pion PDF - II

$$\mathscr{M}(\nu, z^2) = \sum_{n=0}^{\infty} \frac{C_n(\mu^2 z^2)}{C_0(\mu^2 z^2)} \frac{(-i\nu)^n}{n!} a_{n+1}(\mu) + \mathcal{O}(z^2 \Lambda^2_{QCD})$$

- Fit to polynomial of degree m at fixed $z^2$; $1 - \frac{\nu^2}{2!} c_2 + \ldots \frac{\nu^m}{m!} c_m$
- $\langle x^j \rangle_{u-d} = \frac{C_0(\mu^2 z^2)}{C_j(\mu^2 z^2)} c_j$
- Check if divergent logs from fit cancel

C. Shugert

*Ioffe-time moments*

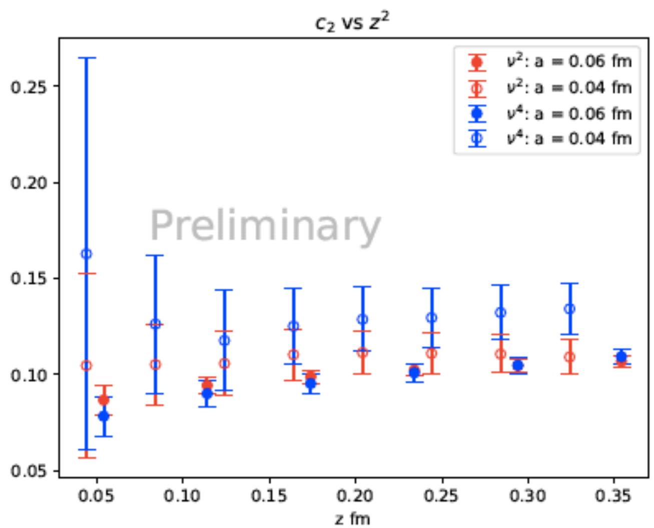


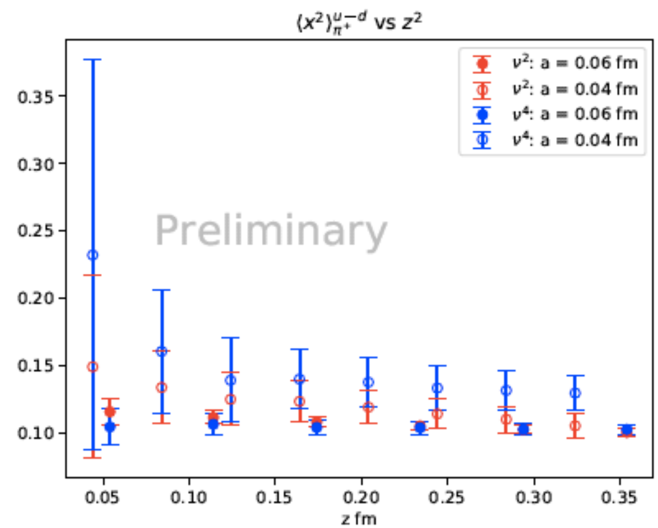

# Hadronic Tensor

**Hadronic Tensor and Neutrino-Nucleon Scattering**

Jian Liang, Terrence Draper, Keh-Fei Liu, Alexander Rothkopf and Yi-Bo Yang
($\chi$QCD collaboration)

J.Liang

## Calculating hadronic tensor on the lattice

$$W_{\mu\nu} = \frac{1}{4\pi}\int d^4z e^{iq\cdot z}\left\langle p,s \left| \left[J_\mu^\dagger(z)\, J_\nu(0)\right] \right| p,s \right\rangle$$

Lattice QCD: **Euclidean** field theory using the path-integral formalism: **time dependent matrix** elements are problematic.

**Minkowski case:**

$$W_{\mu\nu} = \frac{1}{4\pi}\int d^4z e^{iq\cdot z}\left\langle p,s \left| \left[J_\mu^\dagger(z) J_\nu(0)\right] \right| s,s \right\rangle = \frac{1}{2}\sum_n \int \prod_i^n \left[\frac{d^3\mathbf{p}_i}{(2\pi)^3 2E_i}\right] \langle p,s|J_\mu^\dagger(0)|n\rangle\langle n|J_\nu(0)|p,s\rangle(2\pi)^3\delta^4(q-p_n+p)$$

**Euclidean case:**

$$W'_{\mu\nu} = \frac{1}{4\pi}\sum_n \int dt e^{(\nu-(E_n-E_p))t}\int d^3\vec{z} e^{i\vec{q}\cdot\vec{z}}\langle p,s|J_\mu^\dagger(\vec{z})|n\rangle\langle n|J_\nu(0)|p,s\rangle = \frac{1}{4\pi}\sum_n \boxed{\frac{e^{(\nu-(E_n-E_p))T}-1}{\nu-(E_n-E_p)}}\int d^3\vec{z} e^{i\vec{q}\cdot\vec{z}}\langle p,s|J_\mu^\dagger(\vec{z})|n\rangle\langle n|J_\nu(0)|p,s\rangle$$

A simple change from **Fourier transform** to **Laplace transform** in the time direction **leads to divergences when** $\nu-(E_n-E_p)>0$.

Practically, need to solve the **Inverse problem** of the Laplace transform $\tilde{W}_{\mu\nu}(p,q,\tau) = \int d\nu W_{\mu\nu}(p,q,\nu)e^{-\nu\tau}$

**several (O(10)) discrete data points**

**continuous function w.r.t.** $\nu$

**lack of information, an ill-posed problem**

# Hadronic Tensor - II

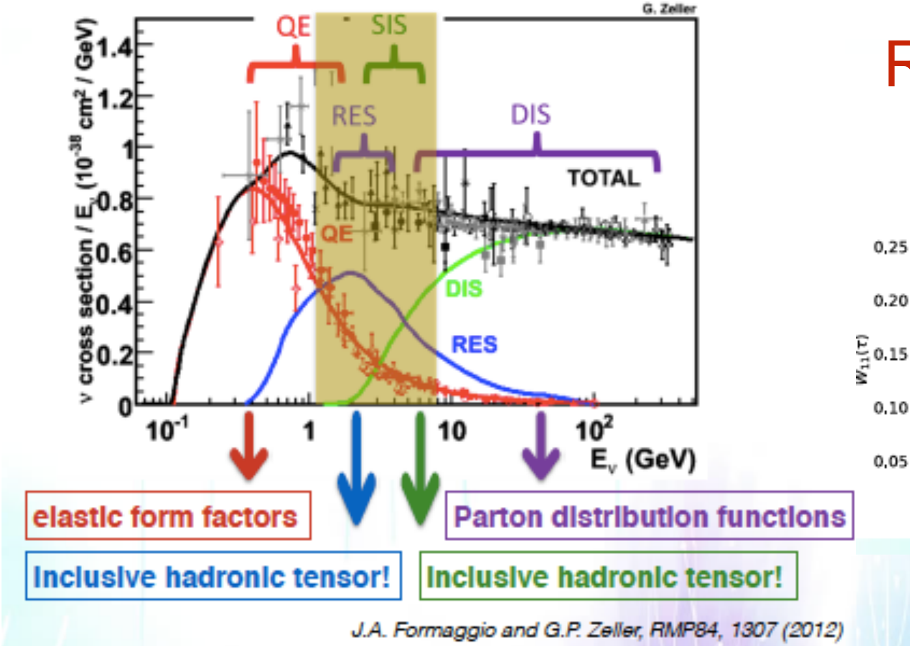


Relevant for DUNE?

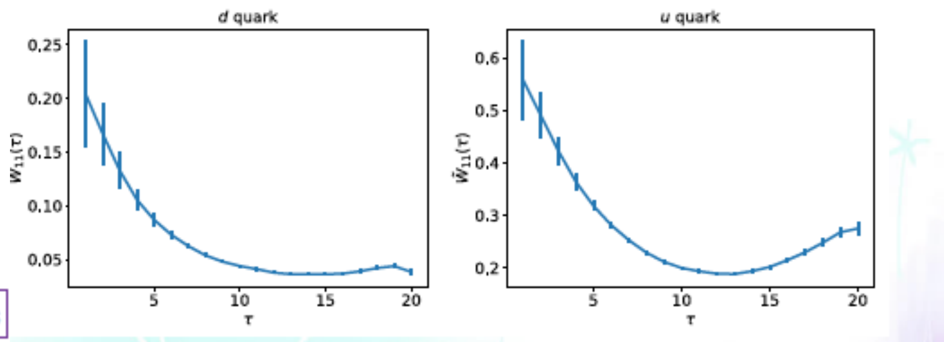


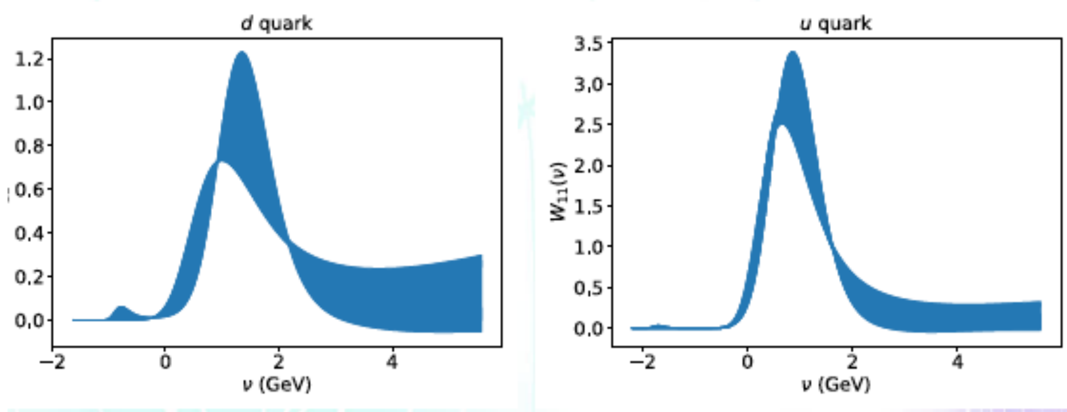

# Scaling and higher twist…

## Scaling and higher twist in the nucleon Compton amplitude


**Ross Young**
University of Adelaide


### Forward Compton amplitude

$$T_{\mu\nu} \sim \int d^4x\, e^{iq.x} \langle p|\mathrm{T} J_\mu(x) J_\nu(0)|p\rangle$$

$$T_1(\omega, Q^2) = \frac{2\omega^2}{\pi}\int_1^\infty d\omega' \frac{\mathrm{Im}\, T_1(\omega', Q^2)}{\omega'(\omega^2 - \omega'^2)} = 4\omega^2 \int_0^1 dx\, x \frac{F_1(x, Q^2)}{1-(\omega x)^2}$$

$$T_1(\omega, Q^2) = \sum_{j=1}^{\infty} 4\omega^{2j} \int_0^1 dx\, x^{2j-1} F_1(x, Q^2) \equiv \sum_{j=1}^{\infty} 4\omega^{2j} f_{1,2j-1}(Q^2)$$

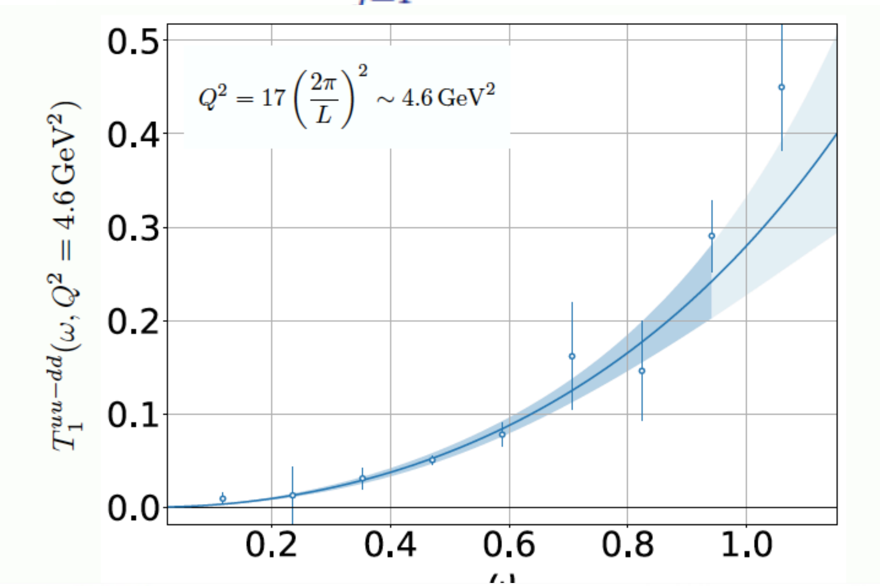


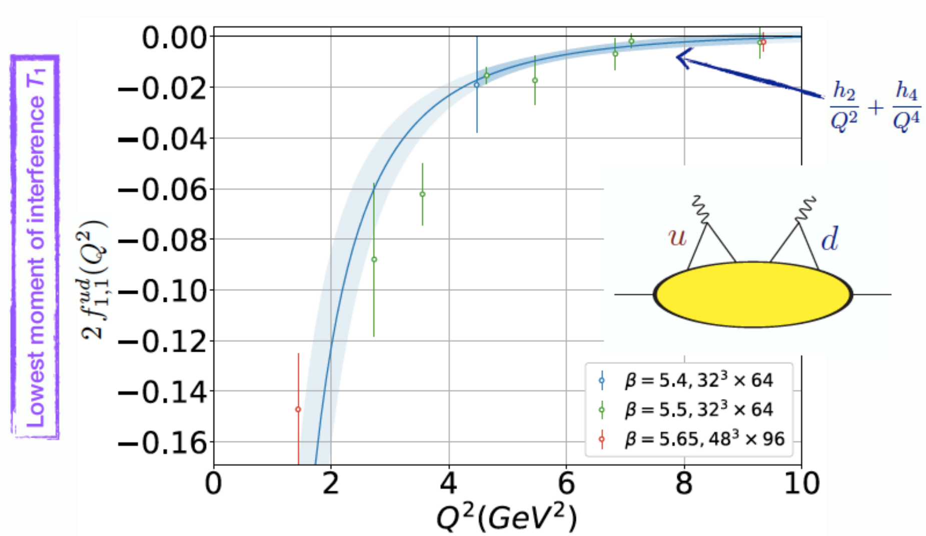

# EicC


**Physics programs and status of EicC**

Yutie Liang

Institute of Modern Physics, CAS, China

On behalf of the EicC Discussion Group

- pRing: figure 8
- 2 interaction regions
- 20GeV p + 3.5 GeV e, $\sqrt{S}$=16.7GeV
- High Lumi.: 2-4 x$10^{33}$ $cm^{-2}s^{-1}$

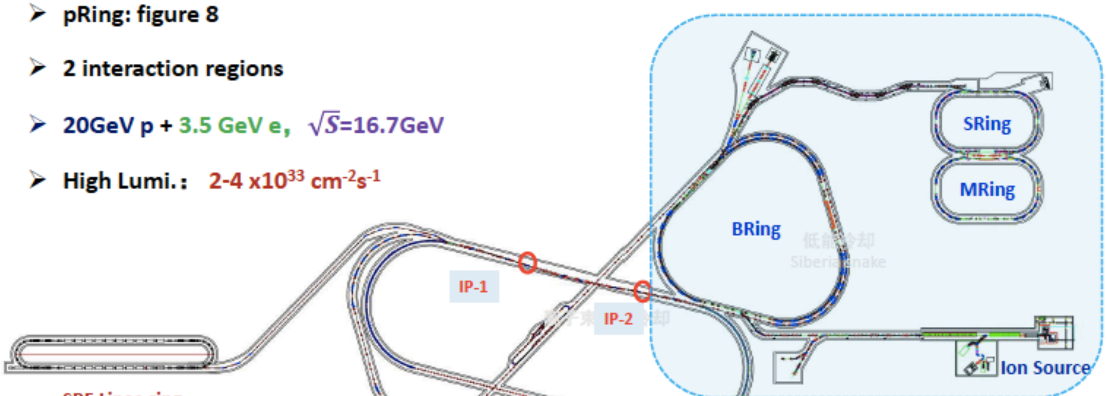

# Computing

Kate Clark

# CHROMA HMC ON SUMMIT

KC, **Bálint Joó**, Mathias Wagner, Evan Weinberg, Frank Winter, Boram Yoon

From Titan running 2016 code to Summit running 2019 code we see >82x speedup in HMC throughput

Multiplicative speedup coming from machine and algorithm

Highly optimized multigrid for gauge field evolution

Mixed precision an important piece of the puzzle

- double – outer defect correction
- single – GCR solver
- half – preconditioner
- int32 – deterministic parallel coarsening

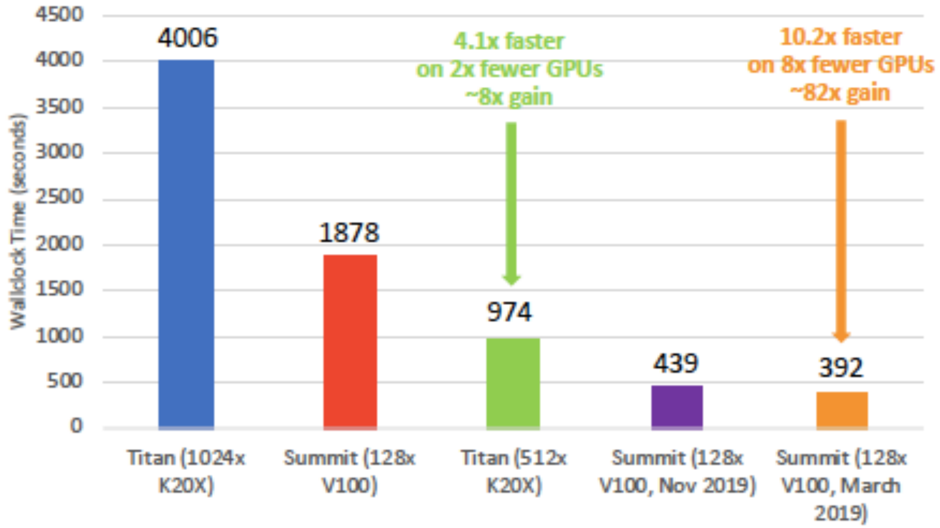

# LATTICE QCD WITH TENSOR CORES

KC, Chulwoo Jung, and Robert Mawhinney, Jiqun Tu

Modern GPU have high throughput tensor-core functionality

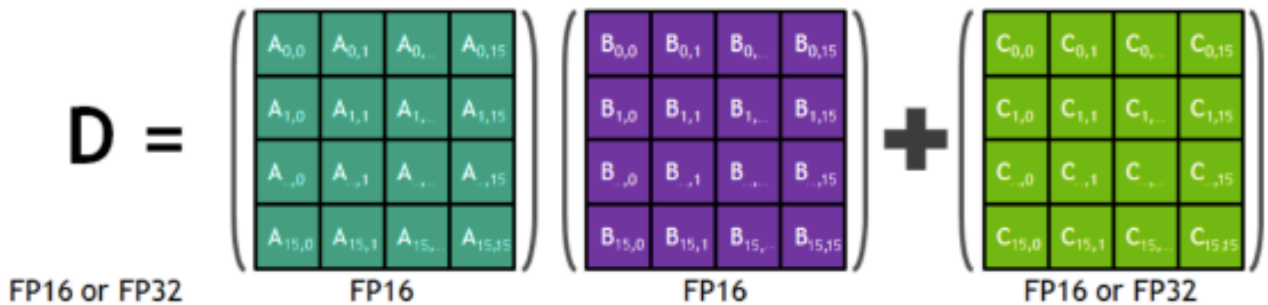


Tesla V100
FP64: 7.5 TFLOPS
FP32: 15 TFLOPS
Tensor: 125 TFLOPS

$$[1-\kappa_b^2 \underbrace{M_\phi^\dagger D_w^\dagger}_{\text{fuse}} \underbrace{M_5^{-\dagger} M_\phi^\dagger D_w^\dagger}_{\text{fuse}} \underbrace{M_5^{-\dagger}][1-\kappa_b^2 M_5^{-1} D_w}_{\text{fuse}} \underbrace{M_\phi M_5^{-1} D_w}_{\text{fuse}} M_\phi]$$

48 NVIDIA

# Supercomputing in China

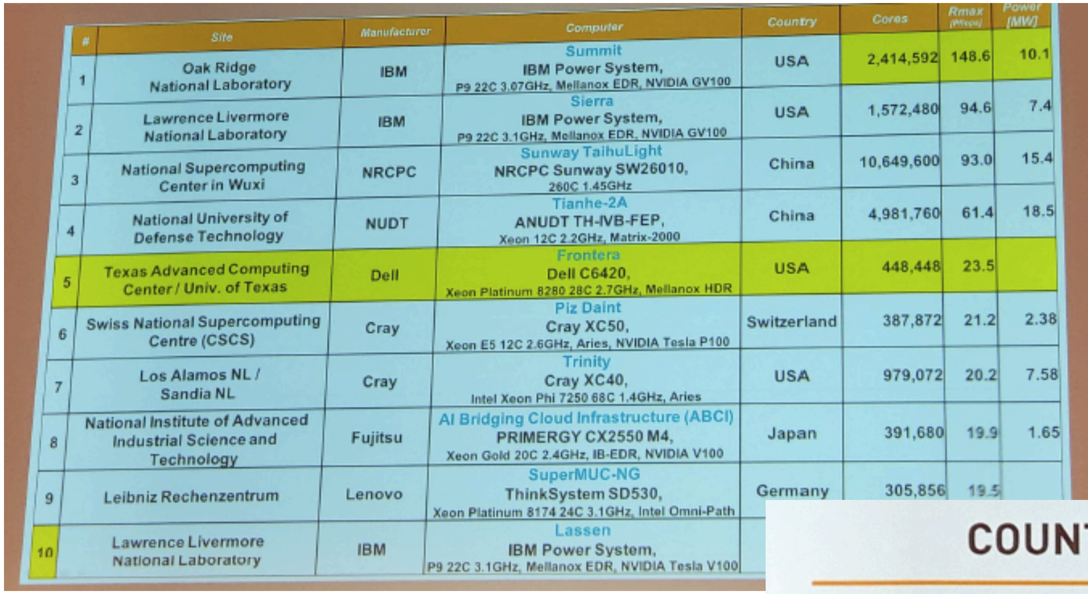

| # | Site | Manufacturer | Computer | Country | Cores | Rmax [Pflop/s] | Power [MW] |
|---|---|---|---|---|---|---|---|
| 1 | Oak Ridge National Laboratory | IBM | Summit IBM Power System, P9 22C 3.07GHz, Mellanox EDR, NVIDIA GV100 | USA | 2,414,592 | 148.6 | 10.1 |
| 2 | Lawrence Livermore National Laboratory | IBM | Sierra IBM Power System, P9 22C 3.1GHz, Mellanox EDR, NVIDIA GV100 | USA | 1,572,480 | 94.6 | 7.4 |
| 3 | National Supercomputing Center in Wuxi | NRCPC | Sunway TaihuLight NRCPC Sunway SW26010, 260C 1.45GHz | China | 10,649,600 | 93.0 | 15.4 |
| 4 | National University of Defense Technology | NUDT | Tianhe-2A ANUDT TH-IVB-FEP, Xeon 12C 2.2GHz, Matrix-2000 | China | 4,981,760 | 61.4 | 18.5 |
| 5 | Texas Advanced Computing Center / Univ. of Texas | Dell | Frontera Dell C6420, Xeon Platinum 8280 28C 2.7GHz, Mellanox HDR | USA | 448,448 | 23.5 | |
| 6 | Swiss National Supercomputing Centre (CSCS) | Cray | Piz Daint Cray XC50, Xeon E5 12C 2.6GHz, Aries, NVIDIA Tesla P100 | Switzerland | 387,872 | 21.2 | 2.38 |
| 7 | Los Alamos NL / Sandia NL | Cray | Trinity Cray XC40, Intel Xeon Phi 7250 68C 1.4GHz, Aries | USA | 979,072 | 20.2 | 7.58 |
| 8 | National Institute of Advanced Industrial Science and Technology | Fujitsu | AI Bridging Cloud Infrastructure (ABCI) PRIMERGY CX2550 M4, Xeon Gold 20C 2.4GHz, IB-EDR, NVIDIA V100 | Japan | 391,680 | 19.9 | 1.65 |
| 9 | Leibniz Rechenzentrum | Lenovo | SuperMUC-NG ThinkSystem SD530, Xeon Platinum 8174 24C 3.1GHz, Intel Omni-Path | Germany | 305,856 | 19.5 | |
| 10 | Lawrence Livermore National Laboratory | IBM | Lassen IBM Power System, P9 22C 3.1GHz, Mellanox EDR, NVIDIA Tesla V100 | | | | |

M. Xiang-Fei

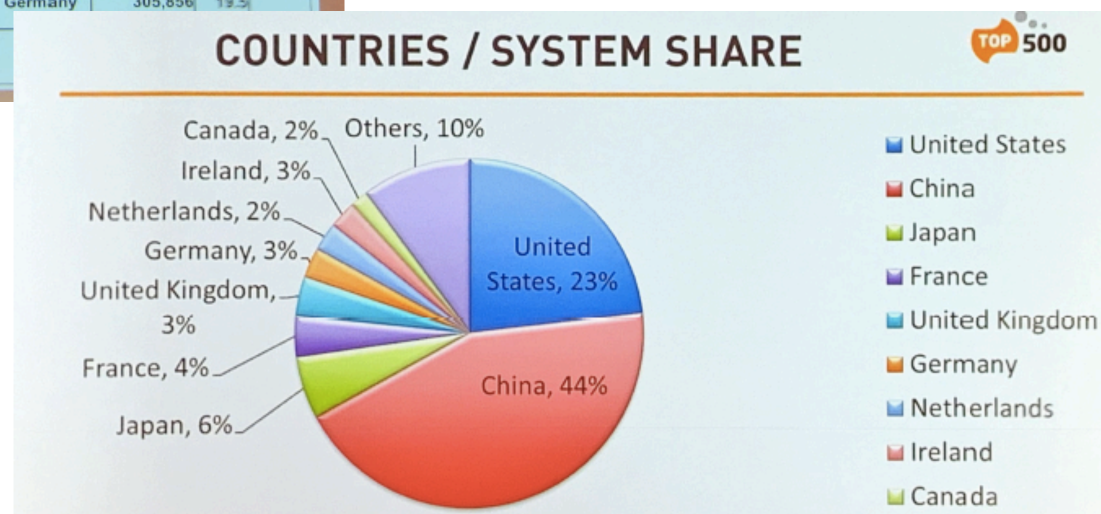

Theoretical Developments,Quantum Computing…

# Tensor Networks

$$Z = \int [d\phi] \exp[iS]$$

$$= \int [d\phi] \prod_x \underline{H_0(\phi_x, \phi_{x+\hat{0}})}\, \underline{H_1(\phi_x, \phi_{x+\hat{1}})}$$

To use tensor network method, path integral should be written in terms of tensor network representation

S. Takeda

$$\underline{H_0(\phi, \phi')} = \exp\left[+\frac{i}{2}(\phi-\phi')^2 - \frac{i}{4}V(\phi) - \frac{i}{4}V(\phi')\right]$$

$$\underline{H_1(\phi, \phi')} = \exp\left[-\frac{i}{2}(\phi-\phi')^2 - \frac{i}{4}V(\phi) - \frac{i}{4}V(\phi')\right]$$

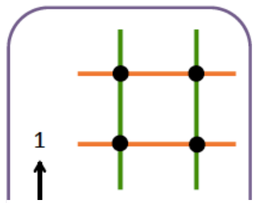


## How to make tensor

For two-variable function

$$H_0(\phi, \phi') = \sum_{k=0}^{\infty} \Psi_k^{(0)}(\phi)\ \sigma_k^{(0)}\ \Phi_k^{(0)*}(\phi')$$

orthonormal basis

singular values

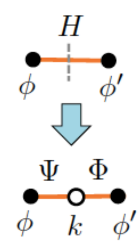


Once the orthonormal basis and singular values are obtained, tensor is formed as

$$T_{ijkl} = \sqrt{\sigma_i^{(0)}\sigma_j^{(1)}\sigma_k^{(0)}\sigma_l^{(1)}} \int_{-\infty}^{\infty} d\phi \Psi_i^{(0)}\Psi_j^{(1)}\Phi_k^{(0)*}\Phi_l^{(1)*}$$

The integral can be estimated by a recursion relation

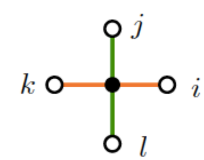

# Tensor Networks - II

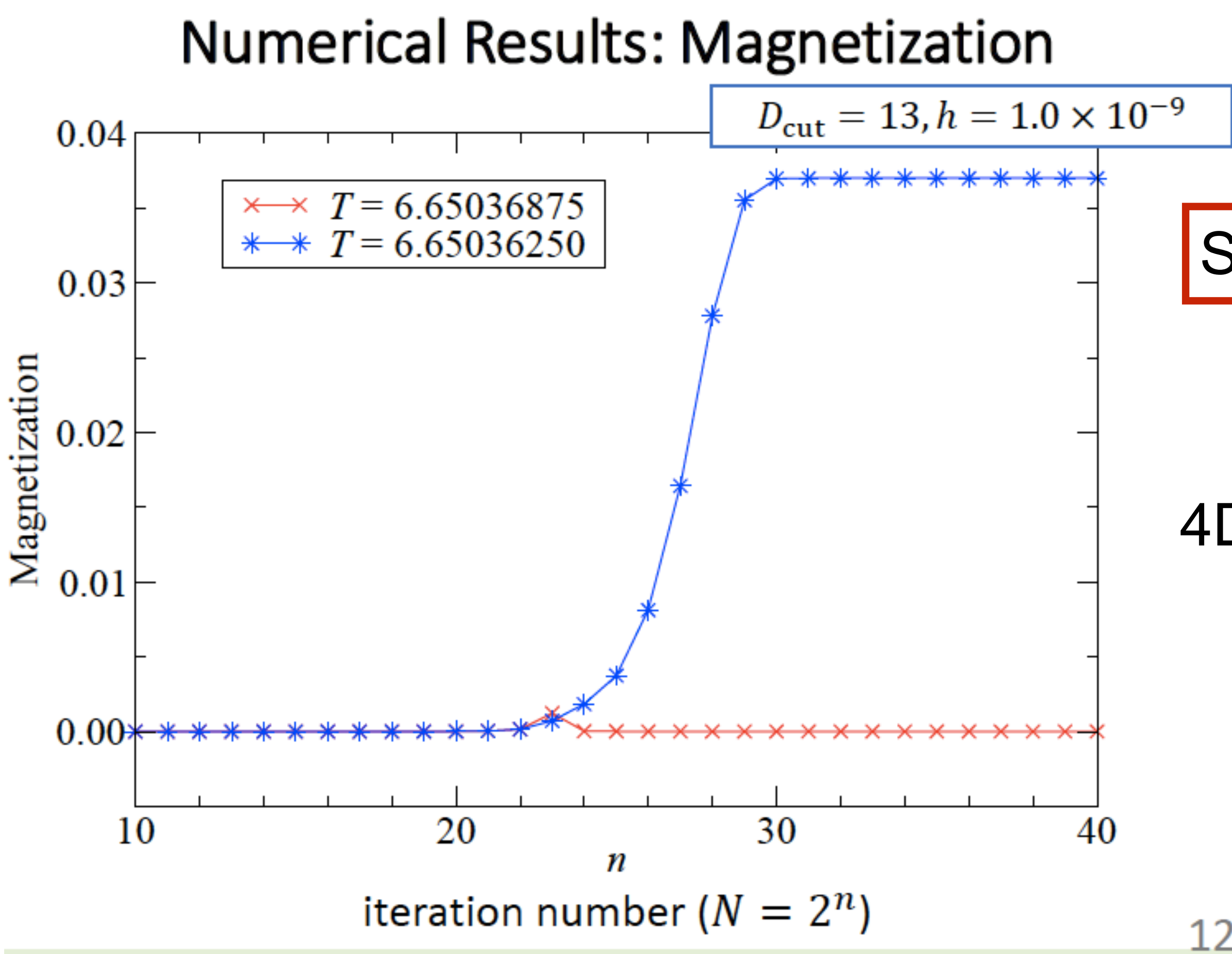


S. Akiyama

4D Ising Model

## Quantum computing zeta regularized vacuum expectation values

K. Jansen

- Feynman's trace formula

$$\langle A\rangle = \lim_{T\to\infty+i0^+} \frac{\mathrm{tr}\{U(0,T)A\}}{\mathrm{tr}\{U(0,T)\}}$$

for a Hamiltonian $H$ (T denoting time ordering)

$$U(0,T) = \mathrm{Texp}\left(-\frac{i}{\hbar}\int_0^T H(\tau)d\tau\right)$$

- allows to formally define trace

**Riemann $\zeta$-function**

- Riemann's $\zeta$-function, $\zeta_{\mathrm{R}}(z)$

$$\zeta_{\mathrm{R}}(z) = \sum_{n=1}^{\infty} \frac{1}{n^z}\ ,\ z \in \mathbb{C}$$

analytical continuation (through $\Gamma$-function)

$\Rightarrow$ well defined for $z \neq 1$

E.g.: choose $z = -1 \rightarrow$ find $\zeta_{\mathrm{R}}(-1) = -\frac{1}{12}$

$$\mathrm{tr}(U(0,T)) = \int dx \int dr \int d\Omega(\xi) e^{ih_2(x,x,\xi)r^2 + ih_1(x,x,\xi)r} a(x,x,r,\xi)$$

$$\begin{aligned}\mathrm{tr}_\zeta(U(0,T)) &= \zeta(k(x,y))(z) \\ &= \int dx \int dr \int d\Omega(\xi) e^{ih_2(x,x,\xi)r^2 + ih_1(x,x,\xi)r} (a\mathfrak{g}(z)(x,x,r,\xi))\end{aligned}$$

| $Q$ qubits | min. eig. $H_Q$ | $\langle \psi_{2Q}, H_Q \psi_{2Q} \rangle$ |
|---|---|---|
| 1 | .392108816647 | .392108816647 |
| 2 | .229395425745 | .229395425968 |
| 3 | .224258841712 | .224258841747 |
| 4 | .223452200306 | .223452200445 |
| 5 | .223336689755 | .223336690423 |

**Variational quantum simulation**

- start with some initial state $|\Psi_{\text{init}}\rangle$
- apply succesive gate operations $\equiv$ unitary operations $e^{-iS\theta}$
- examples for $S$: $\sigma_x$, $\sigma_y$, $\sigma_z$, parametric CNOT

$$|\Psi(\vec{\theta})\rangle = e^{-iS_{(n)}\theta_n} \dots e^{-iS_{(1)}\theta_1} |\psi_{\text{init}}\rangle$$

- with $R_j := e^{-iS_{(j)}\theta_j}$ we obtain cost function

$$C := \left\langle \psi_{\text{init}} \middle| \left(\prod_{j=1}^n R_j\right)^\dagger H \prod_{j=1}^n R_j \middle| \psi_{\text{init}} \right\rangle$$

- goal: minimize $C$ over the angles $\vec{\theta}$
  $\rightarrow$ obtain minimal energy, i.e. ground state
- in original paper:
  - minimization on classical computer
  - minimize over one angle at a time
  - loop several times over the complete set of angle

**Running on the Rigetti hardware**

- Practical example: compute ground state energy of 1-dimensional hydrogen atom on Rigetti's 8-qubit Agave chip
  - performed variational quantum simulation

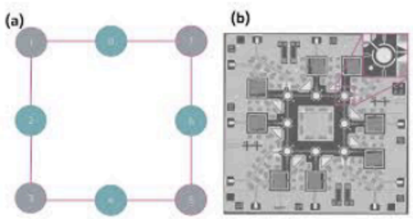


Agave chip

- hardware performance
  - select the qubit of the day
  - found gate fidelity $F_{1Q} = 0.982$ , readout fidelity $F_{RO} = 0.94$
  - ground state energy with $4.9\%$ error
  - more qubits: no significant result

# Opening Talk!

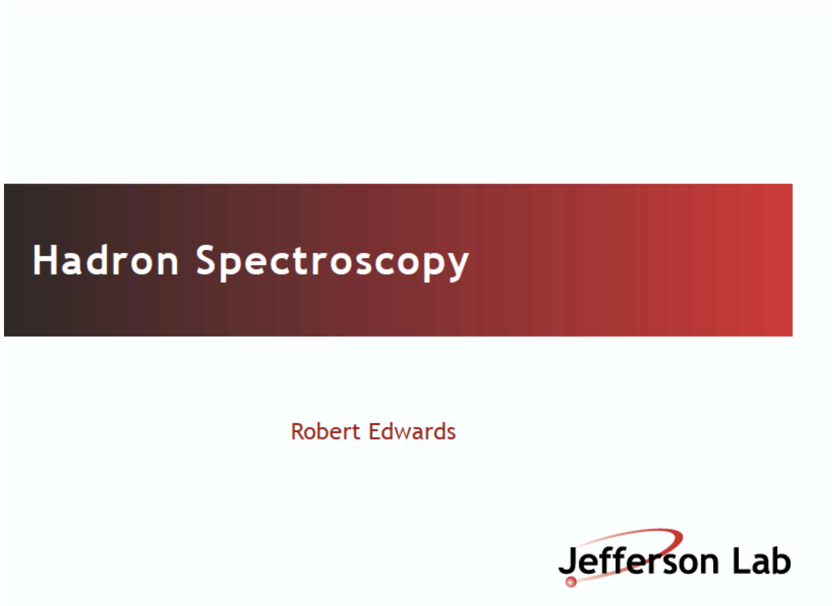


Many plenary on spectroscopy + NN

- Wagman - hadron interactions
- Rusetsky - 3 particles on the lattice
- Gongyo - NN interactions (HALQCD)
- Francis - Tetraquarks

# Summary

- Can’t go to everything, so a lot of topics I haven’t covered…
  - Finite-temperature
  - Weak matrix elements
  - Spectroscopy and NN interactions - lot of plenary talks….
  - BSM
- Hadron Structure Parallel Session
- Lots of references to JLab, both for spectroscopy and structure
  - But others are adopting our methods…..